SECTION I

RESEARCH IN PROGRESS

Comparison of Pre-compound Neutron and Proton Emission in ^{16}O Induced Reactions on ^{238}U at 310 MeV

J. Kasagi, S. Saini, T.C. Awes, A. Galonsky, C.K. Gelbke, G. Poggi, D.K. Scott,
K.L. Wolf[+] and R.L. Legrain[++]

It has been shown that the energy spectra of energetic deuterons and tritons from non-relativistic heavy ion reactions may be related to the energy spectra of protons by a simple coalescence relation with the assumption that protons and neutrons have similar spectral shapes.[1,2] However, a direct comparison of pre-compound proton and neutron cross sections has not yet been performed.

In the present experiment performed at the 88-inch cyclotron of Lawrence Berkeley Laboratory, we measured the neutron and proton energy spectra from ^{238}U + ^{16}O reaction at an incident energy of 310 MeV. A UF_6-target of 320 $\mu g/cm^2$ thickness, mounted on a 80 $\mu g/cm^2$ carbon backing was used. Fission fragments were detected with a surface barrier detector of 60 μm depletion depth and 450 mm^2 active area, mounted at an angle of -90° and at a distance of 1.5 cm from target. Four liquid scintillation detectors (NE 213) were used to detect neutrons emitted at angles of 25°, 40°, 55° and 95°, in coincidence with fission fragments. The flight paths were 2.05 m. In order to reduce the background due to the scattering in the experimental vault, these detectors were placed inside the lead and concrete shields. The remaining background was measured by positioning tapered steel bars of 60 cm lengths halfway between target and detectors and by this means absorbing the neutron originating from the target.

In the off-line analysis, two-dimensional gates were set in the pulse-height versus pulse shape matrices to discriminate γ-rays from neutrons. The neutron detection efficiency was calculated with a computer code originally developed by Kurz.[3] The accuracy of the absolute neutron efficiency was estimated within 15%. The neutron energy was determined with a time-of-flight method. By correcting for the dependence of the neutron-fission timing signal on the energies of the fission fragments, overall time resolution of 1.0 nsec was achieved, resulting in an energy resolution of ±2.5 MeV at 50 MeV.

In the second part of the experiment, coincident protons were detected with two ΔE-E telescopes positioned at the angles of θ_p = 25° and 55°. These telescopes consisted of a 400 μm thick surface barrier detector and a 7.5 cm thick NaI (Tℓ) detector. The detectors were placed outside the scattering chamber which had two exit ports covered with 1 mil mylar windows at these angles.

The differential neutron multiplicities per fission event, $d^2N/N_f dE d\Omega$, are shown in Fig. 1.

In order to facilitate the comparison of proton and neutron cross section, we have decomposed

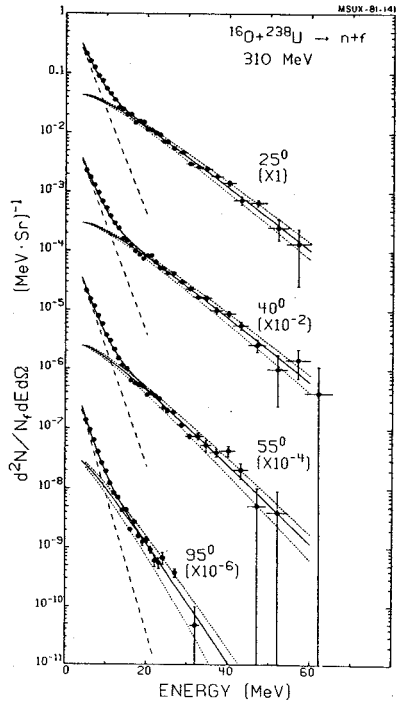

Fig. 1. Differential neutron multiplicities per fission event. The solid and dashed lines show the decomposition into equilibrium and non-equilibrium components, respectively. The dotted lines indicate the estimated errors within which the high energy regions of the neutron spectra are established.

the neutron spectra into an equilibrium and a non-equilibrium component by fitting the energy spectra by the following function:

$$\frac{d\sigma}{dE} = N_o\, e^{-E/T_o} + N_1 \sqrt{E}\, e^{-E/T_1} \qquad (1)$$

where the first term which omits energy factor represents the low energy component and the second term high energy, the non-equilibrium component, and N_o, T_o, N_1, T_1 are adjustable parameters. This decomposition of the spectra is shown in Fig. 1 by the solid and dashed curves. The dotted lines included in the figure show the uncertainties within which the high energy regions of the neutron spectra are believed to be established. The limits defined by these dotted lines will be used for the comparison with the proton cross sections, shown in Fig. 2.

The proton cross sections measured in this experiment are compared to the corresponding neutron cross sections in Fig. 2. The proton data are represented by solid points and the pre-equilibrium neutron components are given by the shaded areas in Fig. 2a. As is apparent from the figure, the shapes of the proton and neutron spectra exhibit significant differences.

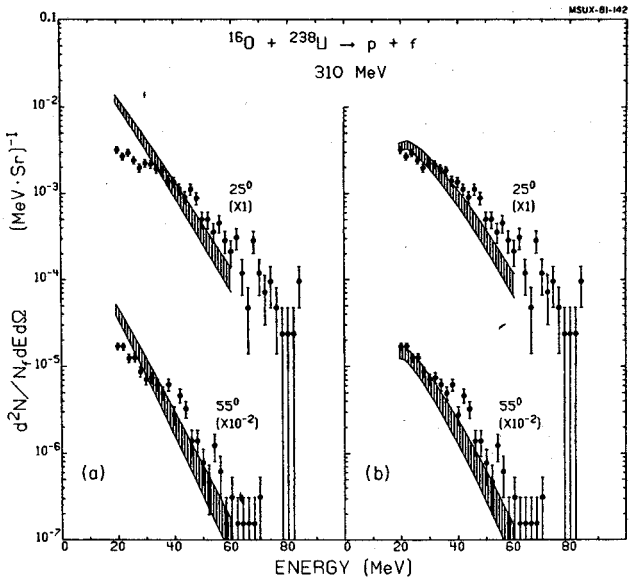

Fig. 2. Differential proton multiplicities per fission event. The shaded areas represent the measured preequilibrium neutron multiplicities (a) and their predicted transformation into proton multiplicities according to eq. 2 of text (b).

The differences in the low energy part of the proton and neutron spectra are most likely due to barrier penetration effects. To illustrate this point, we have transformed the neutron spectra of Fig. 2a according to the relation

$$\frac{d^2\sigma(p)}{dEd\Omega}(E) = \frac{\sigma_R(p)(E)}{\sigma_R(n)(E)} \frac{d^2\sigma(n)}{dEd\Omega}(E) \qquad (2)$$

In eq. (2), the inverse reaction cross sections are calculated from the optical model by using the potentials of ref. 4. The resulting cross sections are shown by the shaded areas in Fig. 2b. Reasonable agreement with the proton cross sections is obtained in the low energy region. The high energy part of the spectrum is, however, only slightly modified.

Our observations show the qualitative trends predicted by recent precompound model calculation of Blann[5] for ^{16}O induced reactions on ^{197}Au at 214 MeV incident energy. A steeper slope is predicted for the (angle integrated) neutron spectrum than for the corresponding proton spectrum.

Recently, it has been shown that the cross sections for the emission of energetic deuterons and tritons may be related to the proton cross sections by a simple coalescence relations.[1,2] This coalescence relation was derived[2] by making the simplifying assumption that the cross sections for pre-equilibrium proton and neutron emission are related as

$$\frac{d^2\sigma_n}{dEd\Omega}(E) = \frac{N}{Z} \frac{d^2\sigma_p}{dEd\Omega}(E-E_c) \qquad (3)$$

In eq. (3), N/Z is the neutron-proton ratio of the compound nucleus. The energy shift E_c was introduced to correct for the final state Coulomb repulsion from the target nucleus. The physics picture implied in eq. (3) is that protons and neutrons have identical kinetic energy distributions at the nuclear surface, where the formation of complex particles takes place. The Coulomb field of the target nucleus merely displaces the energy spectrum of charged particles by the amount of E_c. It is clear from Fig. 2a that eq. (3) is inconsistent with our observations. The low energy neutron cross sections predicted from the proton spectra would be significantly smaller than observed experimentally. The coalescence calculations are quite sensitive to this low energy region - as a consequence, the deutron cross sections are not given by the product of proton and neutron cross sections as determined in this experiment. The success of the coalescence relation given in ref. 2 and possible alternative explanations[6] for the formation of composite light particles remains an interesting subject for future investigations.

---

1. T.C. Awes, C.K. Gelbke, G. Poggi, B.B. Back, B.G. Glagola, H. Breuer, V.E. Viola, Jr., and T.J.M. Symons, Phys. Rev. Lett. 45 (1980) 513.
2. T.C. Awes, G. Poggi, C.K. Gelbke, B.B. Back, B.G. Glagola, H. Breuer and V.E. Viola, Jr., Phys. Rev. C24 (1981) 89.
3. R.J. Kurz, UCRL-11339 (1964).
4. F.D. Becchetti, Jr., and G.W. Greenlees, Phys. Rev. 182 (1969) 1190.
5. M. Blann, Phys. Rev. C23 (1981) 205.
6. F. Hachenberg, H.C. Chiang and J. Hufner, Phys. Lett. 97B (1980) 183.

Light Particle Correlations in 20 MeV per Nucleon ^{16}O Induced Reactions

C.K. Gelbke, W.G. Lynch, L.W. Richardson, M.B. Tsang and R.E. Warner*

The attainment of local thermal equilibrium in heavy ion induced reactions is an important assumption underlying many theoretical models. Until now, light particle correlations testing the thermalization assumption have been measured only at relativistic energies (E/A = 400 and 800 MeV) where the existence of a non-thermal knockout component was demonstrated. In this report, we discuss the first such measurement at non-relativistic energies.

Aluminum and gold targets of 1.6 and 10 mg/cm^2 thickness were bombarded with 310 MeV $^{16}O^{6+}$ ions from the 88 inch cyclotron of the Lawrence Berkeley Laboratory. Single and coincident protons and deuterons were detected with four ΔE-E telescopes consisting of solid state silicon-ΔE and NaI(Tl)-E detectors. The telescopes were mounted in a plane at the angles of -110°, -30°, +30° and +75° with respect to the beam axis, subtending solid angles of 62, 49, 49 and 62 msr, respectively.

We present our results in terms of the correlation function $\sigma_{12}/(\sigma_1\sigma_2)$ where

$$\sigma_{12} = \sigma_0 \int_{\Delta E_1} dE_1 \int_{\Delta E_2} dE_2 \frac{d^4\sigma(\theta_1,E_1,\theta_2,E_2)}{dE_1 dE_2 d\Omega_1 d\Omega_2} \quad (1)$$

and

$$\sigma_k = \int_{\Delta E_k} dE_k \frac{d^2(\theta_k,E_k)}{dE_k d\theta_k} \; ; \; k = 1,2. \quad (2)$$

The constant σ_0 was arbitrarily fixed by requiring $\sigma_{12}/(\sigma_1\sigma_2) = 1$ for the proton-proton correlation corresponding to the variables $\theta_1 = -30°$, $\theta_2 = +30°$, ΔE_1 = 20-40 MeV, and ΔE_2 = 20-100 MeV.

Our experimental results are shown in Fig. 1. The first light particle is defined to be the one detected at $\theta_1 = -30°$. The range of energy integration for the second particle was fixed at ΔE_2 = 20-100 MeV for $\theta_2 = +30°$ and E_2 = 10-100 Mev for $\theta_2 = \pm 100°, \pm 75°$. The error bars shown

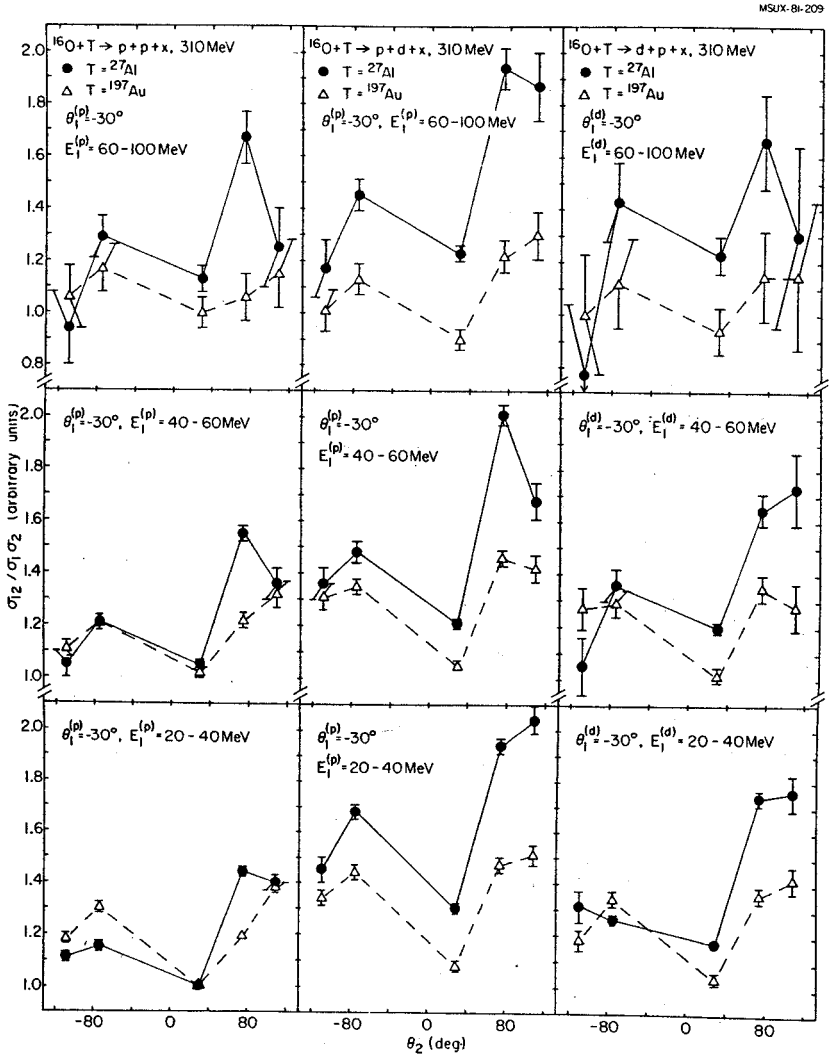

in the figure are purely statistical; systematic errors are believed to be of the order of 5%.

The correlation function exhibits sizable variations which are more pronounced for the Al target than for the Au target. It usually has a minimum value for the forward emission of the second light particle. For the Al target a pronounced left-right asymmetry is observed, corresponding to an enhanced probability for coincident emission of the two light particles on opposite sides of the beam.

For the case of thermal emission from an infinite ensemble the correlation function is constant. However, for nuclear reactions finite particle number effects might not be negligible and variations in the correlation function could be imposed by conservation laws. We have performed simple calculations to investigate the correlations that might be imposed by energy and momentum conservation for a source of A nucleons that emits light particles with a Gaussian momentum distribution. The Galilean-invariant cross section is then given by

$$\frac{d^3\sigma}{dp^3}(\vec{p},\vec{v}_0,T,m) = C(2\pi mT)^{-3/2}\exp\left[-\frac{(\vec{p}-m\vec{v}_0)^2}{2mT}\right] \quad (3)$$

where C is a normalization constant, m is the mass of the emitted particle, T is the temperature parameter and v_0 is the velocity of the source in the laboratory.

The detection of a light particle of laboratory momentum $\vec{p}_1$ and mass m_1 changes the values of both the temperature and the velocity of the remaining ensemble. Denoting $\vec{v}_0'$ and T' as the new source velocity and temperature respectively, the coincidence cross section for the emission of particle 1 of momentum $\vec{p}_1$ followed by the emission of particle 2 of momentum $\vec{p}_2$ is then proprotional to the product

$$P(p_1,p_2) = \frac{d^3\sigma}{dp_1^3}(\vec{p}_1,\vec{v}_0,T,m_1)\,\frac{d^3\sigma}{dp_2^3}(\vec{p}_2,\vec{v}_0',T',m_2). \quad (4)$$

Since experimentally, we cannot distinguish the reverse time sequence, the cross section for the emission of particles 1 and 2 is given by

$$\frac{d^6\sigma}{dp_1^3 dp_2^3} = C_0\left(P(p_2,p_1) + P(p_1,p_2)\right) \quad (5)$$

where C_0 is a normalization constant.

The results of these calculations are compared to the experimental proton-proton correlations for the Al target in Fig. 2. The source parameters of $v_0 = 0.085c$ and T = 6.25 MeV for the Al target were obtained from fits to the singles cross sections.[3] The calculations were arbitrarily normalized to the data at a point which is obvious in the figures. To exhibit the effect of the number of source nucleons on the predicted correlation

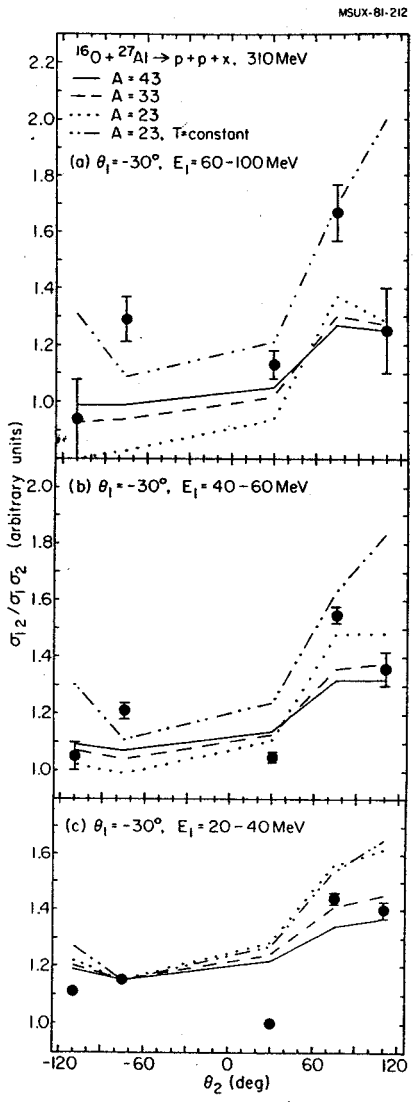

several values of A have been used for the calculations. In addition, one calculation is shown for the case of T = T' = T" (which violates energy conservation for the ensemble but still exhibits the constraints due to momentum conservation).

For the Al target (Fig. 2) the magnitude of the observed left-right asymmetries are comparable to those already predicted for the maximum number of participating nucleons, A = 43. This comparison of calculation with experiment cannot quantitatively determine A since neither the small values of the correlation at $\theta_2 = -30°$ nor the large values at $\theta_2 = -75°$ can be explained by the calculations in a consistent way.

These discrepancies are interesting subjects for future studies with more refined models. Of particular interest is the determination of the influence of impact parameter averaging on the correlation function, and whether the small

values of the correlation function at $\theta_2 = +30^\circ$ can be caused by the presence of low multiplicity peripheral collisions in the singles spectrum at forward angles. Of comparable importance is the calculation of the direct knockout contribution to the correlation as a function of the target mass. Such a component, if present, would be expected to be more important for lighter target projectile combinations and for relative proton laboratory angles close to 90°. This could possibly be related to the enhancement in the correlation at $\theta_2 = +75^\circ$ for the Al target. Moreover, rescattering and absorptive effects (shadowing), especially for heavy target projectile combinations, and possible hydrodynamic effects are of potential interest.

---

* Oberlin College, Oberlin, OH 44074.

1. I. Tanihata, M.-C. Lemaire, S. Nagamiya, and S. Schnetzer, Phys. Lett. 97B (1980) 363.
2. I. Tanihata, S. Nagamiya, S. Schnetzer and H. Steiner, Phys. Lett. 100B (1981) 121.
3. T.C. Awes, G. Poggi, S. Saini, C.K. Gelbke, R. Legrain and G.D. Westfall, Phys. Lett. (in press), and to be published.

Trends of Light Particle Spectra Observed in Nucleus-Nucleus Collisions

T.C. Awes, G. Poggi, S. Saini, C.K. Gelbke, R. Legrain* and G.D. Westfall*

Information about the early stages of heavy-ion induced reactions may be obtained from the detection of energetic light particles which cannot be associated with evaporation from the compound nucleus. At low energies (E/A $\lesssim$ 20 MeV), recent experiments have mainly used coincidence techniques to study detailed aspects of the reaction mechanisms producing energetic light particles. However, few single particle inclusive measurements have been published in this energy domain and little information is available about the dependence of non-compound light particle emission on projectile, target and beam energy. In this communication, we report some of the results obtained from a survey of ^{16}O induced reactions on Al, Zr, and Au targets at 140, 215, and 310 MeV beam energy.

As an example of the general features of the energy spectra that were observed in the present experiment, Fig. 1 shows the results for the $^{197}Au(^{16}O,p)$ reaction for three incident energies. The energy spectra are smooth structureless distributions which, at forward angles, extend to about four times the incident energy per nucleon. With increasing detection angle, the cross sections decrease and the slopes of the energy spectra become steeper.

The cross sections can be rather well described in terms of a Maxwellian distribution observed in a rest frame that moves with a velocity intermediate between target and projectile, see solid curves in Fig. 1. Correcting for the Coulomb repulsion from the target nucleus one obtains non-relativistically[1,2]

$$\frac{d^2\sigma}{dEd\Omega} = N_0(E-E_c)^{\frac{1}{2}}\exp\{-(E-E_c+E_1-2E_1^{\frac{1}{2}}(E-E_c)^{\frac{1}{2}}\cos\theta)/T\} \quad (1)$$

Here, E_c is the kinetic energy gained by the Coulomb repulsion from the target, $E_1=\frac{1}{2}mv^2$ is the kinetic energy of a particle at rest in the moving frame, T is the temperature and N_0 is a normalization constant. The successful application of this parameterization should not be interpreted as evidence for a hot gas of nucleons separated from the target nucleus.[1,2] Rather,

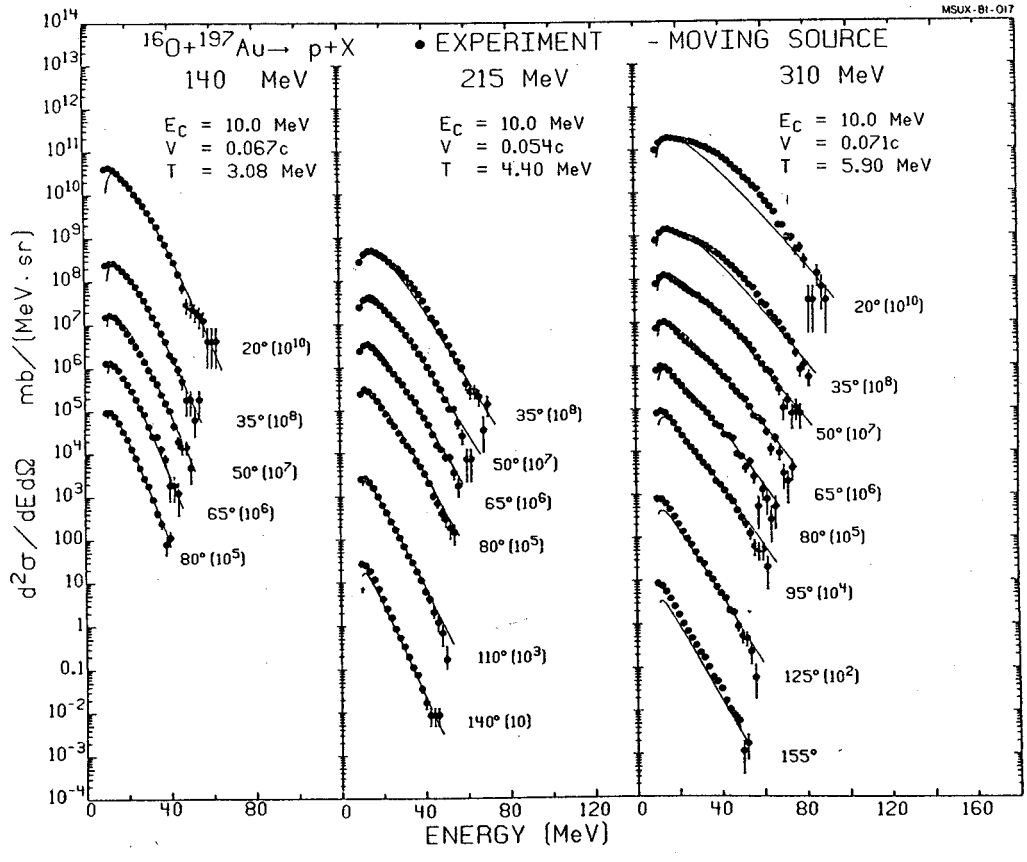

FIGURE 1

Fig. 1. Energy spectra of protons detected in the reaction $^{197}Au(^{16}O,p)$ at incident energies of 140, 215, and 310 MeV. The curves have been calculated with eq. (1) of the text.

it indicates the randomization of light particle velocities in a rest frame that is different from the compound nucleus rest frame. In the present analysis, the values of E_c = 0, 5 and 10 MeV were used for the Al, Zr and Au targets, respectively.

The temperature parameters determined in this experiment are shown in Fig. 2, where they are plotted as a function of $(E-V_c)/A$, the beam energy per nucleon above the Coulomb barrier. For a given type of light particle, the apparent temperatures are approximately proportional to $((E-V_c)/A)^{\frac{1}{2}}$ or, equivalently, proportional to the relative velocity of projectile and target at the point of contact (see insert of Fig. 2). Such a dependence is not expected from compound nucleus emission. It rather suggests more rapid processes such as knockout or, perhaps, the formation of a thermalized subset of nucleons consisting of about equal numbers of target and projectile nucleóns. The deduced values of T are systematically larger for deuterons and tritons than for protons. At present, it is not clear whether this effect could be due to different contributions to the spectra from more equilibrated processes such as compound nucleus evaporation.

The parameterization used to describe our data is similar to the thermal models[3,4] that have been used to describe light particle spectra from relativistic heavy-ion collisons. In order to compare the trends observed at low energies to the ones at relativistic energies, we have determined the temperature parameters for the reaction ^{20}Ne + NaF → p at energies of E/A = 400 and 800 MeV[5] by using the relativistic generalization of eq. (1):

$$\frac{Ed^2\sigma}{p^2dpd\Omega} = N_0\gamma(E-\beta p\cos\theta)\exp(-\gamma(E-\beta p\cos\theta)/T) \qquad (2)$$

where β is the velocity of the source (c = 1), $\gamma = (1-\beta^2)^{-\frac{1}{2}}$ and $E = (p^2 + m^2)^{\frac{1}{2}}$. In order to minimize the contribution from projectile fragmentation and knockout[5] we have restricted the data to large transverse momenta ($\theta \geq 45^o$) for the determination of T. Despite the simplicity of the parameterizaton, the fits are of acceptable quality. The resulting temperature parameters are included in Fig. 2.

As is obvious from Fig. 2, the trends observed at low energies can be connected in a smooth fashion

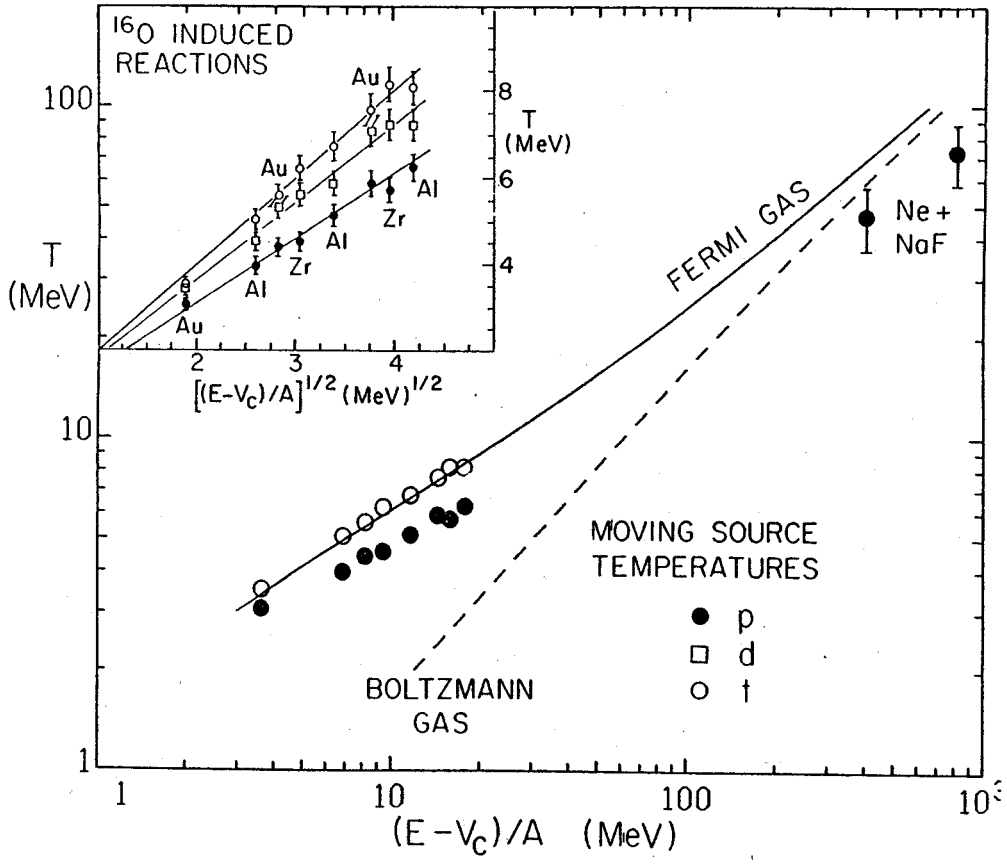

FIGURE 2

Fig. 2. Temperature parameters for proton, deuteron, and triton spectra in ^{16}O induced reactions on targets of Al, Zr, and Au at incident energies of 140, 215, and 310 MeV and for the reaction Ne + NaF → p at 400 and 800 MeV/A. The solid and dashed curves are explained in the text.

to the observations at high energies. For orientation, the solid and dashed curves have been calculated for relativistic Fermi and Boltzmann gases consisting of equal nucleon contributions from target and projectile.

The general trend of the experimental temperature parameters is seen to follow the one depicted by the Fermi gas curve. Although the observed trends suggest the thermalization of a subset of nucleons it should also be investigated whether alternative approaches such as single or multiple nucleon scattering models or hydrodynamical models would predict similar trends.

---

* Lawrence Berkeley Laboratory, Berkeley, Ca 94720.

1. T.C. Awes, C.K. Gelbke, G. Poggi, B.B. Back, B. Glagola, H. Breuer, V.E. Viola, Jr., and T.J.M. Symons, Phys. Rev. Lett. 45 (1980) 513.
2. T.C. Awes, G. Poggi, C.K. Gelbke, B.B. Back, B. Glagola, H. Breuer, and V.E. Viola, Jr., Phys. Rev. C24 (1981) 89.
3. G.D. Westfall, J. Gosset, P.J. Johansen, A.M. Poskanzer, W.G. Meyer, H.H. Gutbrod, A. Sandoval, and R. Stock, Phys. Rev. Lett. 37 (1976) 1202.
4. J. Gosset, J.I. Kapusta, and G.D. Westfall, Phys. Rev. C18 (1978) 844.
5. S. Nagamiya, M.C. Lemaire, E. Moeller, S. Schnetzer, G. Shapiro, H. Steiner, and I. Tanihata, Lawrence Berkeley Laboratory Report LBL-12123, to be published, and private communication.

Energy Dependence of Light Particle Production from High Energy Heavy Ion Collisions

G.D. Westfall, N. Anantaraman, M. Curtin, G.M. Crawley, C.K. Gelbke, B. Hasselquist, B. Jacak, R. Legrain, W.G. Lynch, T.J. Majors, M.J. Murphy, D.K. Scott, T.J.M. Symons and B.M. Tsang

The energy dependence of light particle production can be used to study the basic differences in the way nuclei interact at low energies and very high energies. The study of projectile fragmentation has demonstrated the rapid onset of fragmentation at incident energies, E_{inc}, near the Fermi momentum E_f[1]. For light particle production, one might expect a similar effect in excitation functions of observables including the temperature in the center of mass frame, the velocity of any identifiable emitting sources and the ratios of p, d, t, ^{3}He, and ^{4}He production cross sections to those of protons.

The systems studied in the present work include ^{20}Ne + Al, Au and ^{40}Ar + Ca, U at 100 and 156 MeV/nucleon. Beams of approximately 10^7 particles/second from the Low Energy Beam Line at the LBL Bevalac were used. Energy spectra and angular distributions were measured for p, d, t, ^{3}He, and ^{4}He from 30° to 130° using a variety of detector telescopes. The experimental arrangement for the Ne induced measurements is shown in Fig. 1. Two heavy ion telescopes were installed at ± 10° in the laboratory and were capable of measuring energy spectra of projectile-like fragments for Ne to Li isotopes. Targets consisted of 100 mg/cm^2 Al and Au mounted at 50° to the beam. Singles and coincidence measurements were acquired simultaneously for all nine telescopes. To facilitate calibration of the telescopes, beams of 50, 100, 150 MeV/nucleon p were used as well as using overlapping angular settings of adjacent telescopes to cross compare the measured energy spectra.

The energy spectra of protons and deuterons from ^{20}Ne + Au at 100 MeV/nucleon are shown in Fig. 2 for θ_{lab} = 50, 70, 90, 110 and 130°. Note that the low energy component (≤30 MeV) is nearly isotropic in the laboratory. The solid lines represent a calculation of spectra from a source moving at a third the projectile velocity and having a temperature of 32 MeV for protons and deuterons corresponding to the systematics of Awes et al.[2]

Preliminary results for d/p and ^{4}He/p ratios for Ne + Au at 100 and 150 MeV/nucleon are shown in Fig. 3 along with data at lower and higher energies.[2,3,4,5] Note that the d/p ratio hardly

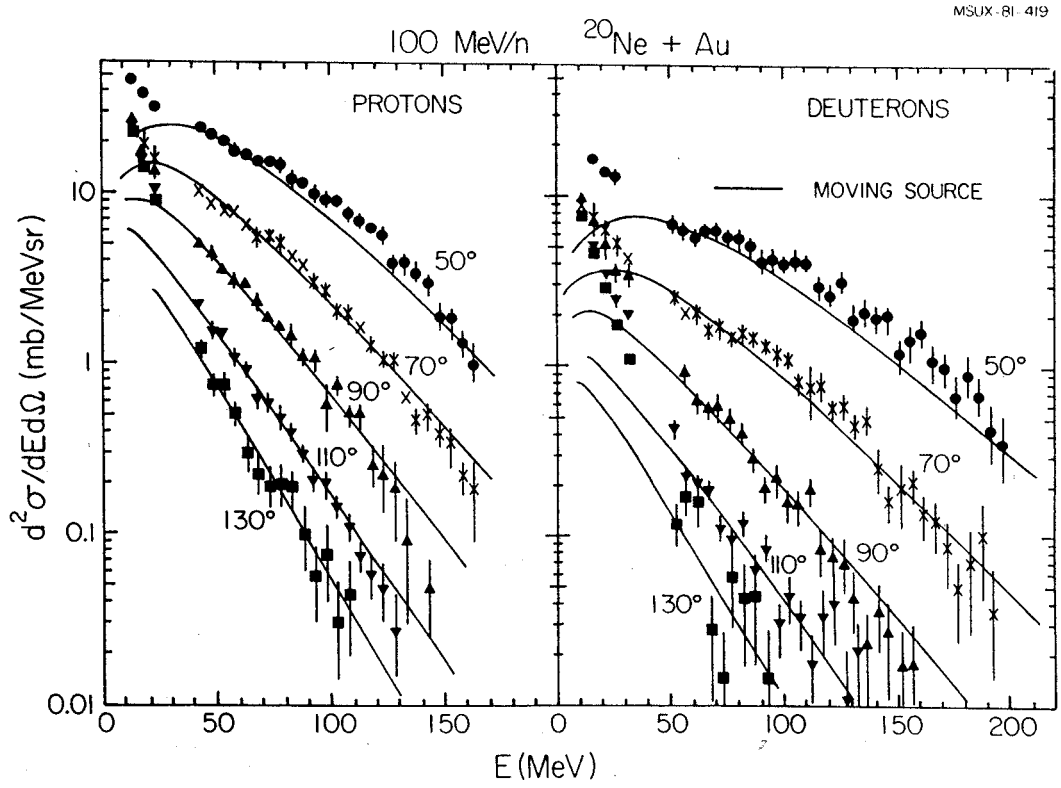

Fig. 2. Spectra of protons and deuterons from 100 MeV/n ^{20}Ne + Au. The 30° spectra are not shown.

MSUX-81-414

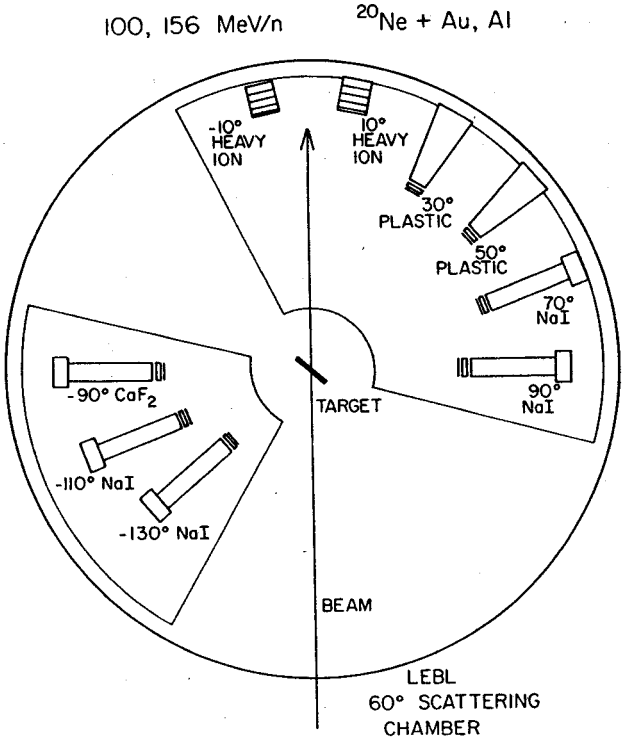

Fig. 1. Experimental layout showing the seven light ion telescopes at angles from 30 to 130° and the two heavy ion telescopes each at 10°.

changes from 20 to 2000 MeV/nucleon while the ^{4}He/p ratio changes by about a factor of 20. These preliminary data hint strongly that a transition takes place as one varies the incident energy above energies of 20 MeV/nucleon.

MSUX-81-457

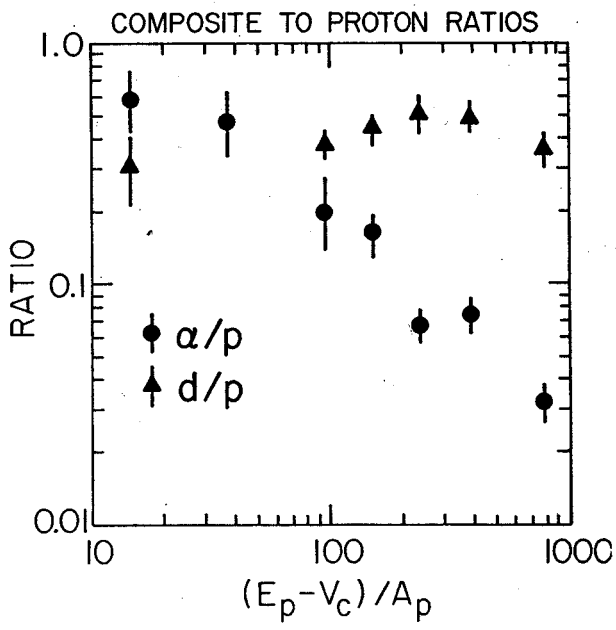

Fig. 3. Composite to proton ratios as a function of incident energy per nucleon above the Coulomb barrier.

1. D.K. Scott, Nucl. Phys. A354, 375 (1981).
2. T.C. Awes, G. Poggi, S. Saini, C.K. Gelbke, R. Legrain, and G.D. Westfall, MSU preprint MSUCL-351 (1981) and Phys. Lett. B to be published.
3. J. Gosset, H.H. Gutbrod, W.G. Meyer, A.M. Poskanzer, A. Sandoval, R. Stock, and G.D. Westfall, Phys. Rev. C16, 629 (1977).
4. J.B. Natowitz, M.N. Namboodiri, L. Adler, R.P. Schmitt, R.L. Watson, S. Simon, M. Berlanger, and R. Choudhury, Texas A&M Preprint (1981).
5. S. Nagamiya, M.C. Lemaire, E. Moeller, S. Schetzer, G. Shapiro, H. Steiner, and I. Tanihata, LBL-12123 (1981), and to be published in Phys. Rev.

Center-of-Mass Velocity Pions Produced in Heavy Ion Collisions

W. Benenson, G.M. Crawley, E. Kashy, J.A. Nolen, K.A. Frankel,* J.A. Bistirlich,* R. Bossingham,* H.R. Bowman,* K.M. Crowe,* C.J. Martoff,* D. Murphy,* J.O. Rasmussen,* J. Sullivan,* W.A. Zajc,* J.P. Miller,+ O. Hashimoto,** M. Koike,** J. Peter,*** and J. Quebert****

An experiment was undertaken at the Bevalac to study the peak observed by Wolf et al.[1] in the π^+ spectrum taken at E/A = 1.05 GeV, ^{40}Ar + Ca. This peak or ridge occurs at $p_\perp = 0.5\ m_\pi c$ and $p_{//}^{cm} = 0$ and was attributed to possible hydrodynamic flow effects. In the present experiment both π^+ and π^- were detected to check the idea proposed by theorists[2] that the peak is a Coulomb effect due to the charged remnants of the reaction.

Since the data have seen recently submitted for publication (LBL-12585), we present here only a brief summary of the results. The data only overlap a small region of the results of Wolf et al., but this region is a critical one in that it includes the rise of the cross section from $p_\perp = 0$ out to $0.5\ m_\pi c$. Figure 1 shows contour plots created by feeding to a computer program the data of ref. 1 alone and combined with ours. The dotted lines show the region studied in the present experiment. Reflections of the data about $p_{//}^{cm} = 0$ are also used to draw contour lines. The present data show that the ridge of ref. 1 is in fact a plateau which is consistent with some theoretical models for the reaction mechanism.

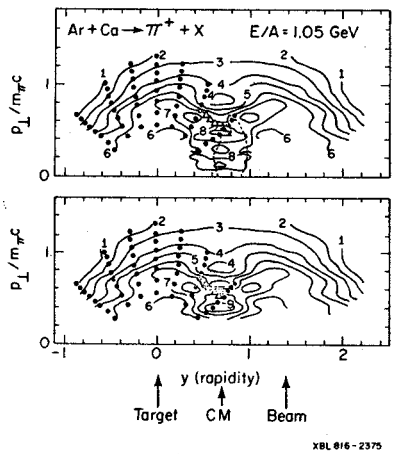

Fig. 1. Countour plots of π^+ invariant cross sections for ^{40}Ar + Ca at E/A = 1.05 GeV. The dots show the data points of ref. 1, and dashed line encloses the region of the present data. The lower half shows the data of ref. 1 alone, and the upper half includes the present data. Contours are at intervals of $1\mu b\text{-}sr^{-1}\text{-}MeV^{-2}$.

Of particular interest is the π^-/π^+ ratios near $p_{//}^{cm} = 0$. These are most sensitive to the charge remnants, for example a fireball in the center-of-mass frame, and are calculated to be of the order 3-5. Figure 2 gives the π^- and π^+ spectra for three targets at $\theta = 20^o$. The π^-/π^+ ratio for ^{40}Ar + Ca is almost independent of $p_\perp$ and averages 1.7 ± 0.2. This ratio can be explained completely by the Coulomb effects of target and projectile fragment and the neutron excess of the beam. In other words no charge at rest in the center-of-mass frame is required to fit the data. However, recent theoretical calculations with realistic boundary conditions in which the pions are created at the surface of the fireball are also consistent with the data.

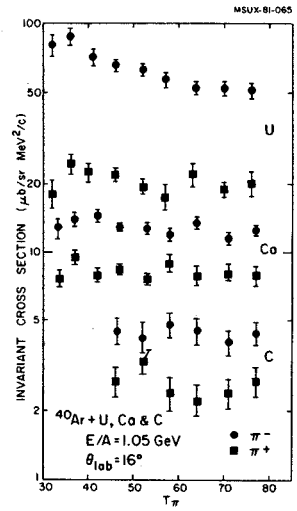

Fig. 2. Comparison of π^+ and π^- cross sections at 20° for E/A = 1.05 GeV ^{40}Ar on U, Ca and C.

* LBL and Boston University.
** INS Tokyo
*** IPN Orsay
**** University of Bordeaux.

1. K.L. Wolf, H.H. Gutbrod, W.G. Meyer, A.M. Poskanzer, A. Sandoval, R. Stock, J. Gosset, C.H. King, Nguyen Van Sen, and G.D. Westfall, Phys. Rev. Lett. 42, 1448 (1979).
2. K.G. Libbrecht and S.E. Koonin, Phys. Rev. Lett. 43, 1581 (1979) and M. Gyulassy and S.K. Kauffmann, Nucl. Phys. A362, 503 (1981).

Fragmentation of ^{40}Ar at 118 MeV/nucleon

G.D. Westfall, R. Legrain, T.C. Awes, H.J. Crawford, C.K. Gelbke, D.E. Greiner, H.H. Heckman, J.M. Kidd, P.J. Lindstrom, J. Mahoney, D.K. Scott, A.C. Shotter and T.J.M. Symons

In recent years, experiments studying the fragmentation of high energy heavy ions have established the basic features of these reactions.[1-3] Heavy fragments are observed near the beam velocity with a momentum distribution which is nearly isotopic in the projectile rest frame. Isotope production cross sections and the associated transverse and longitudinal momentum widths are essentially independent of the beam energy and the target, except for the absolute magnitude of the cross sections which scale with the reaction cross sections. Many of these general features can be described by a variety of models including direct break-up, excitation and sequential decay, abrasion - ablation and intranuclear cascade. The fragmentation of ^{40}Ar at 118 MeV/nucleon was chosen to complement measurements with light projectiles near 100 MeV/nucleon and to extend previous measurements of ^{40}Ar and ^{48}Ca fragmentation near 200 MeV/nucleon that exhibited most of the features established for reactions up to 2 GeV/nucleon.

Using a beam of 118 MeV/nucleon ^{40}Ar from the Lawrence Berkeley Laboratory Bevalac with an intensity of about 10^6 particles/second, measurements were made at 0.5° intervals out to 8°. The detection system consisted of four lithium-drifted silicon ((Si(Li)) detectors. The first detector was 1 mm thick and the next three were 4.75 mm thick. The targets were ^{232}Th and ^{12}C of 149 mg cm^{-2} and 80.8 mg cm^{-2} thickness respectively. The targets and detector telescope were placed in the large vacuum tank of the zero-degree spectrometer. Energy spectra and angular distributions were measured for Al to Cl isotopes. In Fig. 1 the energy spectra are shown for ^{38}Cl and ^{36}S isotopes from ^{40}Ar + ^{12}C at 1° in the lab. The solid lines correspond to a gaussian momentum distribution in the projectile rest frame with the form

$$\frac{d^3\sigma}{dp_{11}dp_\perp} = \frac{1}{\sigma_{p_{11}}} \exp\left[\frac{-(p_{11}-\langle p_{11}\rangle)^2}{2\sigma_{p_{11}}^2}\right] \frac{1}{\sigma_{p_\perp}} \exp\left[\frac{-p_\perp^2}{2\sigma_{p_\perp}^2}\right]$$

where p_{11} is the parallel momentum, $\sigma_{p_{11}}$ is the parallel momentum width, $\langle p_{11}\rangle$ is the parallel momentum shift, $\sigma_{p_\perp}$ is the perpendicular momentum, and $\sigma_{p_\perp}$ is the perpendicular momentum width. The angular distributions of these isotopes are shown in Fig. 2 for ^{40}Ar + C and Th along with the gaussian fits.

The results of fitting the spectra for all the observed isotopes are given in Fig. 2. Note that the $\sigma_{p_\perp}$ are substantially larger than $\sigma_{p_{11}}$ for the Th target while they are comparable for the ^{12}C target. This effect has been explained in terms of an orbital dispersion model.[4]

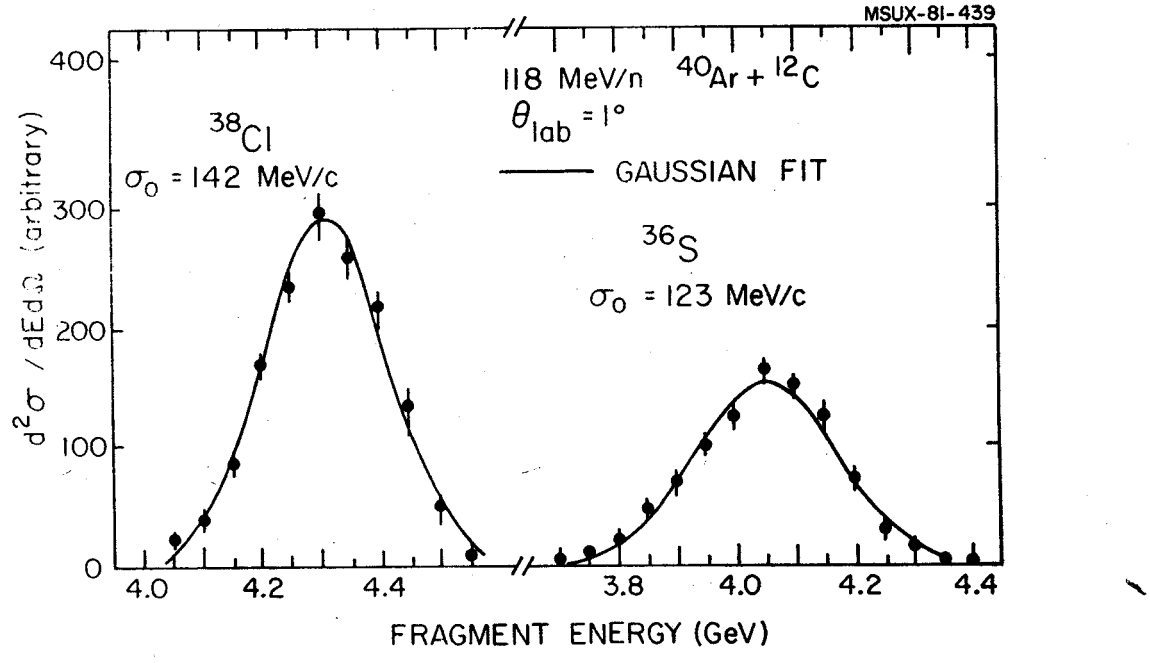

Fig. 1. Energy spectra of ^{36}S and ^{38}Cl isotopes at 1° in the laboratory for 118 MeV/nucleon ^{40}Ar + ^{12}C. The solid line corresponds to a gaussian fit as described in the text.

Note the strong banding in the $\sigma_{p_{11}}$ for the isotopes of a given element. We have qualitatively reproduced this effect using an abrasion-ablation type model incorporating momentum widths and shifts. In addition, the fact that the widths are substantially less than one would expect from known systematics is explained by the model. Excited "prefragments" having relatively narrow widths decay by light particle emission giving rise to the observation of fragments farther from the projectile mass. These fragments exhibit the narrower width of the parent, heavier fragments. Introduction of friction into the model will allow the prediction of parallel momentum shifts.

1. D.E. Greiner, P.J. Lindstrom, H.H. Heckman, Bruce Cork, and F.S. Bieser, Phys. Rev. Lett. 35, 152 (1975).
2. P.J. Lindstrom, D.E. Greiner, H.H. Heckman, B. Cork, and F.S. Bieser, Lawrence Berkeley Laboratory Report No. LBL-3650, 1975.
3. Y.P. Viyogi, T.J.M. Symons, P. Doll, D.E. Greiner, H.H. Heckman, D.L. Hendrie, P.J. Lindstrom, J. Mahoney, D.K. Scott, K. Van Bibber, G.D. Westfall, H. Wieman, H.J. Crawford, C. McParland, and C.K. Gelbke, Phys. Rev. Lett. 42, 33 (1979).
4. K. Van Bibber, D.L. Hendrie, D.K. Scott, H.H. Wieman, L.S. Schroeder, J.V. Geaga, S.A. Chessin, R. Truehaft, Y.J. Groissiord, J.O. Rasmussen and C.Y. Wong, Phys. Rev. Lett. 43, 840 (1979).

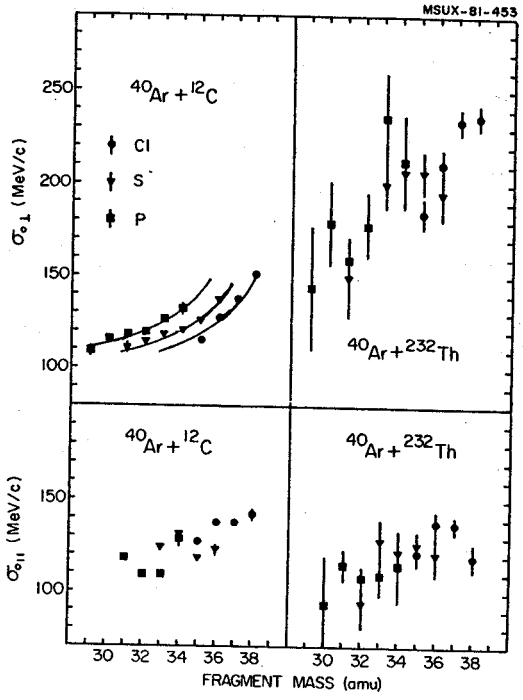

Fig. 2. Reduced parallel and perpendicular momentum widths for 118 MeV/nucleon $^{40}Ar + ^{12}C$ and ^{232}Th for P, S, and Cl isotopes. The solid lines are drawn to guide the eye.

Systematics of Isotope Production Cross Sections for Ar Induced Reactions on ^{100}Mo and ^{232}Th Targets

L.H. Harwood, T.C. Awes, C.K. Gelbke, J.A. Nolen, W. Bohne,* K. Grabisch* and C. Morgenstern*

Over the past decade, vast amounts of experimental effort have been put into the study of deeply inelastic reactions. Unfortunately, absolute isotopic differential cross sections are seldom published. More rare are the instances where cross sections are reported for multiple angles, bombarding energies, and/or targets as part of one experiment. Thus, reliable analysis of systematic dependences are difficult to make. Therefore, the present work was undertaken. The measurements were made at the Hahn-Meitner Institute (Berlin) with the VICKSI accelerator. Isotope production cross sections were measured for an ^{40}Ar beam an ^{100}Mo and ^{232}Th targets at various scattering angles and beam energies. The beam energies and scattering angles are listed in Table I. The reaction products were measured with a ΔE-E-time-of-flight counter system which gave complete isotope and element identification for A≲55 and Z≲26 in this experiment.

Table I. Targets, Bombarging Energies and Observation Angles used in this Study.

Target	Energy (MeV)	Angle
^{100}Mo	280	15°,20°,25°
	387	13.5°,18°,23°
^{232}Th	387	18°,23°,30°,33°

For deeply inelastic reaction products (i.e. completely relaxed kinetic energies in the exit

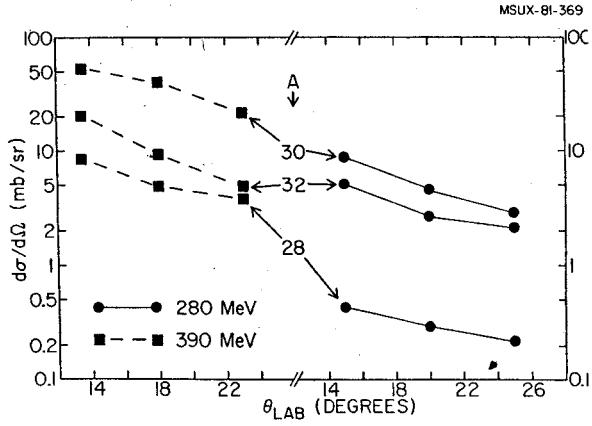

Fig. 1. Angular distributions for production of silicon isotopes in ^{40}Ar + ^{100}Mo reactions.

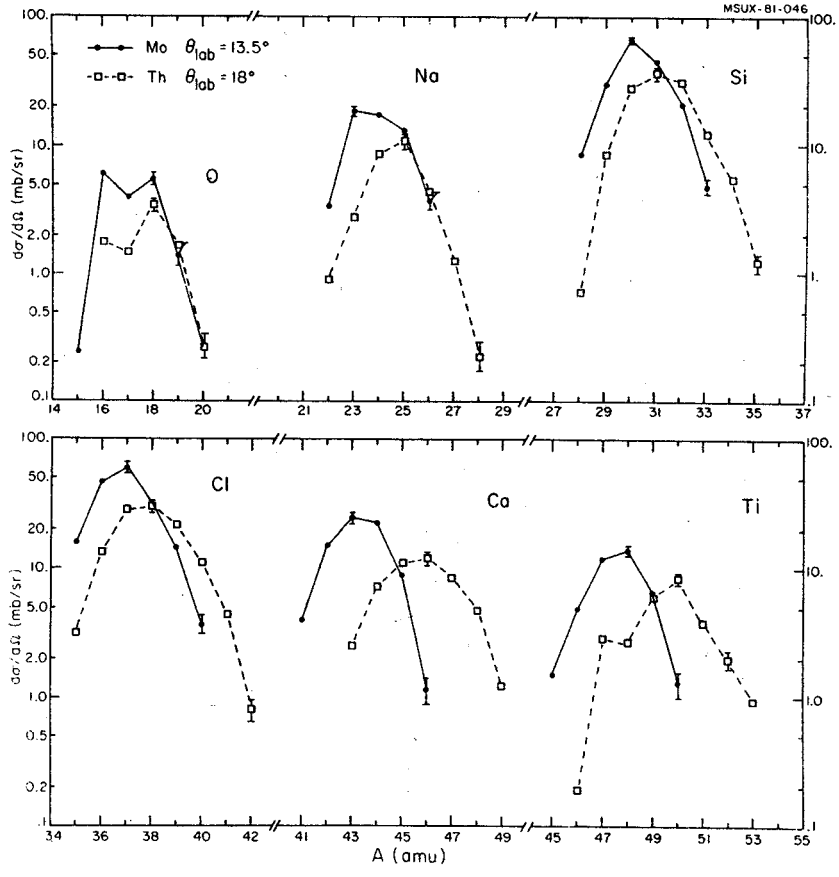

Fig. 2. Energy-integrated isotopic cross sections for a ^{40}Ar beam at 390 MeV. Results for ^{100}Mo and ^{238}Th targets are shown.

channel), the isotopically summed elemental cross sections are very similar for the two targets and showed no significant angular dependence. There were however significant angular, energy, and target effects seen in the isotopic cross sections. Cross sections decreased monotonically as the scattering angle increased. This is illustrated in Fig. 1. Typically the decrease was about a factor of two for each 7° change in angle.

The effects of the target on isotopic cross sections are illustrated in Fig. 2. The angles were chosen so that the systems were observed at approximately equal deflections from the respective grazing angles. The isotopic cross sections are similar for the two targets for the O isotopes. As the product's Z increases, the similarity for the two targets decreases. While the overall magnitude of the cross sections are similar and the shape of the $\frac{d\sigma}{d\Omega}$ vs A curve for a given element is similar for the two targets, there is a shift in the peak of the distributions between the two targets. More to the point, for heavier ejectiles, e.g. Ca, the thorium target had much larger cross sections for the heavier isotopes. The converse was true for the lighter isotopes of all elements. This is consistent with the increased N/Z ratio for the Th target.

Figure 3 compares the cross sections for Si and Ca isotopes for $^{40}Ar + {}^{100}Mo$ at 280 MeV and 387 MeV bombarding energies. While the data are not at the same scattering angles, the angular distribution data (see Fig. 1) indicate a 20% upward correction of the 280 MeV data would make up for the difference. After this correction the data for Ca are quite similar for the two energies. On the other hand, the cross sections for Si isotopes at 387 MeV are much larger than those at 280 MeV. These observations are not unexpected as there is more energy available at the higher bombarding energy for driving the system away from the entrance channel. Thus, the elemental production for isotopes different than the beam should become larger as the bombarding energy increases. This effect should increase as the final system becomes more dissimilar from the initial system. Gratifyingly, we observe a small effect for the Ca isotopes ($\Delta Z=2$) and a larger effect for the Si isotopes ($\Delta Z=4$).

One of the reasons for this study was to better enable predictions of the optimum energy,

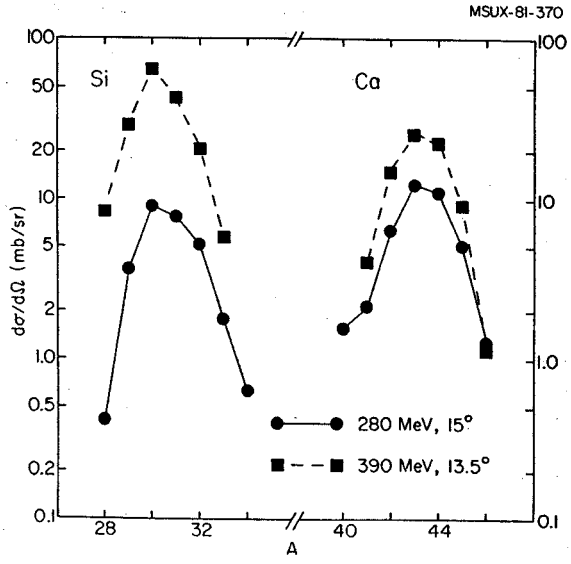

Fig. 3. Illustration of the effects of beam energy on isotopic production cross section.

target and angle for production of exotic nuclei. With the present results the following guidelines arise:

1. A decrease in angle increases the yield (about a factor of 2 for a 7° shift);
2. heavier targets increase the yield of neutron rich isotopes;
3. an increased bombarding energy also increases the yields.

The next step in the study should be to try different beams on a given target.

We note in passing that no neutron deficient nuclei were observed; from this we conclude that deeply inelastic reactions are a poor way of making such nuclei. Our results are somewhat inconclusive on this point however since both the targets and beam had $N/Z > 1$. This is another reason for investigating with a different beam.

---

* Hahn Meitner Institute, Berlin

The Fusion Mechanism of the $^{12}C+^{16}O$ Reaction

F. Haas, A. Galonsky, J. Kasagi, B. Remington, J. Kolata,* P. de Young,*
L. Satkowiak,* M. Xapsos,* R. Freeman,* F. Prosser,** and R. Racca**

The excitation function for the total fusion cross section (σ_F) of the $^{12}C+^{16}O$ reaction at bombarding energies above the Coulomb barrier presents the following two features:

Structures have been observed in σ_F[1]. The main contribution to these structures comes from the fusion channels involving at least one α particle.[2]

This observation indicates that resonant behavior is correlated with angular momenta in the entrance channel close to the grazing angular momentum L_g.

As for other light heavy-ion systems,[3] σ_F increases sharply at energies above the Coulomb barrier and then, above $E_{c.m.} \simeq 21$ MeV for $^{12}C+^{16}O$, levels off to stay at an almost constant value. The origin of this saturation is still an open question (entrance channel and/or compound nucleus effects).

To describe the saturation it is generally assumed that the entrance channel angular momenta between L_c, the critical angular momentum for compound nucleus formation, and L_g do not contribute to the fusion mechanism.

The above features are closely related to entrance channel angular momentum effects for which there exists only indirect evidence. The aim of the present experiments is to get a more direct insight into these angular momentum considerations for the $^{12}C+^{16}O$ reaction. The experiments performed so far at the University of Notre Dame tandem accelerator can be briefly described as follows:

- In all experiments the fusion channels have been selected through their characteristic γ-rays observed in a Ge(Li) detector placed at $\theta_\gamma = 55^o$;
- The average γ-ray energy associated with each fusion channel was measured. The energies were deduced from γ rays observed in a collimated NaI (9"ϕ x 4") counter in coincidence with γ transitions seen in the Ge(Li) detector;
- The γ-ray multiplicities of the individual fusion channels were deduced from measurements of coincident γ rays recorded in an array of six NaI (6"ϕ x 3") detectors.

From the analysis of these two experiments, for which data have been obtained at seven bombarding energies between $E_{c.m.} = 18$ and 26 MeV (this energy range covers the two main features of σ_F described above), we expect to deduce the entry line for the $^{12}C+^{16}O$ reaction for several fusion channels as a function of bombarding energy.

---

* University of Notre Dame
** University of Kansas

1. P. Sperr, S. Vigdor, V. Eisen, W. Henning, D.G. Kovar, T.R. Ophel and B. Zeidman, Phys. Rev. Lett. 36, 405 (1976).
2. J.J. Kolata, R.M. Freeman, F. Haas, B. Heusch, and A. Gallmann, Phys. Lett. 65B, 333 (1976); Phys. Rev. C19, 408 (1979).
3. D.G. Kovar, D.F. Geesamain, T.H. Braid, Y. Eisen, W. Henning, T.R. Ophel, M. Paul, K.E. Rehm, S.J. Sanders, P. Sperr, J.P. Schiffer, S.L. Tabor, S. Vigdor, B. Zeidman and F.W. Prosser, Jr., Phys. Rev. C20, 1305 (1979).

Resonant Structure in ^{14}C Induced Reactions

F. Haas

The resonant structure in light heavy-ion reactions has been under extensive study for the last twenty years. However until recently the structure observed in the excitation functions of integrated reaction channels was confined to collisions involving ^{12}C and/or ^{16}O. A complete review of all the published data before 1977 can be found in Ref. 1.

The first extensive study of a ^{14}C induced reaction at bombarding energies well above the Coulomb barrier was reported by Freeman et al.[2] who observed strong and completely unexpected structure in reaction channels of the $^{12}C+^{14}C$ reaction. The excitation functions of the inelastic channel corresponding to the $^{14}C(3^-)$ state at 6.73 MeV and of the neutron transfer channel to the $^{13}C(5/2^+)$ at 3.85 MeV are shown on Fig. 1. The cross sections of these reaction channels have been measured through γ-ray techniques and a complete description of the experimental techniques can be found in Ref. 3. Very similar results have been obtained by Kolata et al.[4] for the $^{14}C+^{16}O$ reaction. In that case, the strongest direct reaction channels were the α and/or the 2n transfer channels to the 2^+ and 4^+ excited states in ^{18}O. The pronounced and correlated resonant structure observed in the summed and individual excitation functions of these channels is shown on Fig. 2.

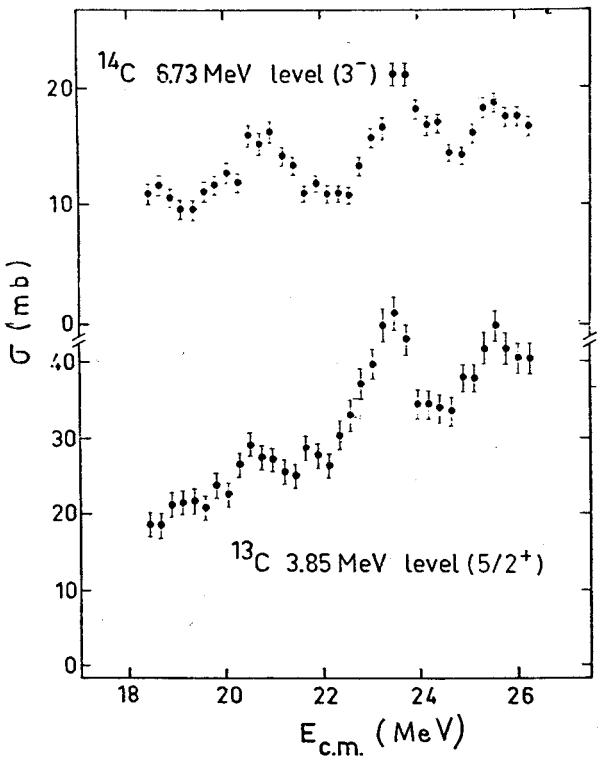

The surprising results obtained for the $^{12}C+^{14}C$ and $^{14}C+^{16}O$ reactions have prompted a large experimental effort to study the $^{14}C+^{14}C$ scattering of the identical bosons. Elastic scattering data have now been published by the Munich and Los Alamos groups[5] at bombarding energies between $E_{C.M.}$ = 6 to 35 MeV. The most interesting feature of this data is a pronounced and periodic gross structure in the $\theta_{C.M.} = 90^o$ excitation function, which is very similar to earlier results obtained by the Yale group[6] for the $^{16}O+^{16}O$ reaction. The study of the $^{14}C+^{14}C$ reaction has been completed very recently[7] by measurement of the reaction channels excitation functions. It was found that resonant structure was not only present in the direct reaction channels (inelastic and transfer) but also in some fusion channels and especially in the αxn to Ne isotopes.

All the mentioned results for the ^{14}C induced reactions are very similar to those reported previously for the $^{12}C+^{16}O$ and $^{16}O+^{16}O$ systems. This similarity clearly emphasizes the identical role played by the ^{16}O and ^{14}C nuclei to provide the ideal conditions for resonant structure observation. Such a conclusion based on experimental observations is confirmed by recent calculations of Haas and Abe[8] where the number of open reaction channels for all these systems have been calculated as a function of bombarding energy. The calculations show a strong similarity of the surface transparent interaction in ^{16}O and ^{14}C induced reactions.

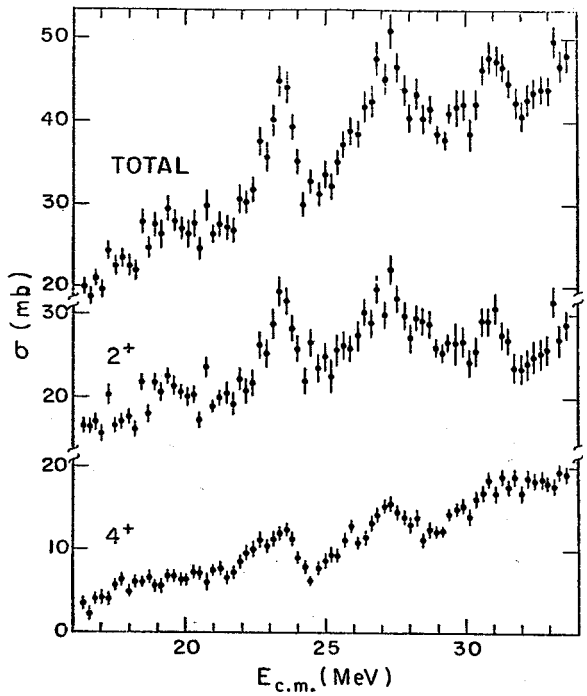

This transparency is a consequence of the closed or semi-closed shell structure of these nuclei, and as a result there is only a small number of open reaction channels able to carry away the higher entrance channel angular momenta at bombarding energies well above the Coulomb barrier.

The formation mechanism of the resonant structure in light heavy-ion reaction is still an open question (molecular, barrier top resonances, diffraction effects...) but the latest results obtained for the ^{14}C induced reactions confirm that a necessary condition to observe resonances is a weak absorption surface transparent interaction.

---

1. Nuclear Molecular Phenomena, edited by N. Cindro (North-Holland, Amsterdam, 1978).
2. R.M. Freeman et al., Phys. Lett. 90B, 229 (1980).
3. J.J. Kolata, et al., Phys. Rev. C19, 408 (1979).
4. J.J. Kolata, et al., Phys. Rev. C23, 1056 (1981).
5. D. Konnerth, et al., Phys. Rev. Lett. 45, 1154 (1980); D.M. Drake, et al., Phys. Lett. 98B, 36 (1981).
6. J.V. Maher, et al., Phys. Rev. 188, 1665 (1969).
7. Strasbourg-Munich collaboration, Phys. rev. (to be published).
8. F. Haas and Y. Abe, Phys. Rev. Lett. 46, 1667 (1981).

Two-particle Exclusive Reactions for $^{24}Mg+^{24}Mg$

F. Haas, R.R. Betts,* B.B. Back,* S. Saini,* B.G. Glagola,* I. Ahmad,*
J. Yntema* and R.W. Zurmühle**

A high resolution study of two-particle exclusive reactions produced in the $^{24}Mg+^{24}Mg$ collision has been started at the Argonne National Laboratory Tandem-Linac accelerator. A ^{24}Mg target of ~40 $\mu g/cm^2$ thickness was bombarded with a ^{24}Mg beam (charge state 7^+ and intensity 10 to 30 nA). The kinematics of the reaction were used to identify the masses of the outgoing nuclei and to improve the energy resolution needed to resolve individual final states of the produced nuclei. To achieve these goals experimentally, the energies and angles of coincident reaction products were measured with two position sensitive Si surface-barrier detectors placed at $\theta = 45^o$ on each side of the beam axis and subtending solid angles of 30 and 100 msr, respectively. Data were taken at bombarding energies of 68 MeV and from 70 to 130 MeV in 5 MeV steps. An on-line analysis of the excitation function of all coincident events, including two-body final states and also more complex states, shows a sharp decrease of cross section with a minimum at a bombarding energy of 85 MeV followed by a cross section increase. From the different mass spectra, it can be deduced that the inelastic scattering channels dominate at all energies over reactions in which particles are transferred. The energy spectra of inelastically scattered nuclei show in the 75-100 MeV bombarding energy range a selective population of multiple excitation of yrast states in both fragments with strong feeding of ^{24}Mg yrast states up to the 8^+ levels.

---

* Argonne National Laboratory
** University of Pennsylvania

The (^{14}N,^{10}B) Reactions on ^{24,26}Mg at 83 MeV

A.F. Zeller, L.H. Harwood, R.E. Tribble,* Y.-W. Lui,* and N. Takahashi*

Shell model predictions for alpha-spectroscopic factors between ground states for the Mg-S systems[1] are in agreement with light ion (α,2α) results[2] but are inconsistant with heavy ion induced reactions.[3-5] In order to try to understand this problem, the (^{14}N,^{10}B) reaction was studied on ^{24,26}Mg at 83 MeV. The ^{26}Mg(^{14}N,^{10}B)^{30}Si reaction has been shown[6] to be adequately described by DWBA calculations at 70 MeV, giving an indication that the reaction mechanism is direct. An earlier study of the relative ground state spectroscopic factors of the two reactions at 70 MeV proved inconclusive due to insufficient statistics;[7] thus the present measurements were undertaken.

Beam currents of up to 1.5 μA were obtained from the Texas A&M 88" cyclotron and were used to bombard targets of isotopically enriched ^{24}Mg and ^{26}Mg on thin carbon backings. Data were taken at lab angles of 8°, 9° and 10°. Reaction products were observed in the focal plane of an Enge split-pole spectrograph using a 1.2 m detector[8] with mass and change identification obtained from energy loss information. Unfortunately, the mass resolution was insufficient to completely resolve ^{10}B and ^{11}B. The yields for the ^{26}Mg(^{14}N,^{10}B)^{30}Si(g.s.) were thus obtained with large uncertainties because of leak-through from the much more intense ^{26}Mg(^{14}N,^{11}B)^{29}Si reaction. Several states were observed in the ^{24}Mg reaction, however. The results are shown in Fig. 1. Absolute cross sections have an estimated uncertainty of ±40%, due mainly to the normalizations to forward angle elastic scattering.

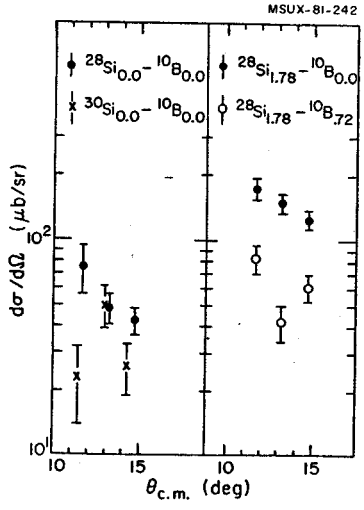

Fig. 1. Cross sections to states populated in the ^{24,26}Mg(^{14}N,^{10}B)^{28,30}Si reactions at 83 MeV. Subscripts refer to the excitation energy of the levels in Si and B.

It is observed that the cross sections for the two ground state transitions are essentially equal. Since Q values, and hence angular momentum matching, are nearly equal for the ^{24}Mg and ^{26}Mg channels, it is unlikely that the elastic scattering and DWBA predictions differ significantly. This implies that the relative alpha-spectroscopic factors are nearly equal, in agreement with theory[1] and the (α,2α) results[2] but in disagreement with other heavy ion alpha-transfer results summarized in Table I. This disagreement between the (^{14}N,^{10}B) reaction and the other heavy ion reactions is puzzling since the DWBA fits to the ^{26}Mg(^{14}N,^{10}B)^{30}S reaction at 70 MeV implies a direct mechanism. However, the fact that other "conventional" alpha-transfer reactions give such dissimilar spectroscopic factors for the two Si ground states, leads one to the conclusion that the (^{14}N,^{10}B) reaction has a reaction mechanism significantly different from the other reactions. The simplest explanation is that the (^{14}N,^{10}B) reaction is a sequential transfer of 2p-2n. This would suggest that the added two neutrons in ^{26}Mg block easy transfer of an alpha-particle vis a vis ^{24}Mg. Further studies using such unusual transfers as (^{13}C,^{9}Be) or (^{18}O,^{14}C) should be used to further study this problem.

Table I. Cross section ratios for α-transfer reactions on ^{24,26}Mg.

Reaction (Energy)	$\frac{d\sigma}{d\Omega}(^{26}Mg)/\frac{d\sigma}{d\Omega}(^{24}Mg)$	ref
(^{6}Li,d) 36 MeV	0.16[a]	3
(^{12}C,^{8}Be) 50 MeV	0.1[b]	4
(^{16}O,^{12}C) 42 MeV	0.029	5
(^{14}N,^{10}B) 83 MeV	0.62±.30	present study

[a] Ground state of ^{30}Si reported as "small". We have assigned an arbitrary upper limit of 10μb/sr for this state.
[b] The ground state was not observed in the ^{30}Si spectrum. The strongest state in the ^{30}Si spectrum was used here.

* Cyclotron Institute, Texas A&M University, College Station, TX 77843

1. W. Chung, et al., Phys. Lett. 79B, 381 (1978).
2. J.D. Sherman, D.L. Hendrie and M.S. Zisman, Phys. Rev. C13 20 (1976).
3. J.P. Draayer et al., Phys. Lett. 53B, 250 (1974).
4. E. Mathiak et al., Nucl. Phys. A259, 129 (1976).
5. J.V. Maher et al., Phys. Rev. Lett. 29, 29 (1972).
6. A.F. Zeller, et al., Nucl. Phys. A301, 130 (1978).
7. A.F. Zeller, et al., BAPS 24, 572 (1979) (unpublished).
8. N. Takahashi et al., "Progress in Research 1979-1980", Cyclotron Inst., Texas A&M Univ., p. 95 (unpublished).